Prepublished copy

Nature Environment & Pollution Technology

This is a peer-reviewed prepublished version of the paper

Original Research, Review

FLASH FLOOD SUSCEPTIBILITY MAPPING USING GEOSPATIAL AND ANALYTICAL HIERARCHY PROCESS MODELING - A STUDY OF WADI HABBAN BASIN, SHABWAH, YEMEN

Haial Al-kordi[1], Abdulmohsen Al-Amri[2] and Govinda raju [2†]

[1]Research Scholar, Department of Applied Geology, Kuvempu University, Jnanasahyadri, Shankaraghatta, Shivamogga, Karnataka - 577451, India; h9975001259@gmail.com

[2]Professor, Department of Engineering Geology, Shabwah University, Ataq city, Shabwah Governate, Yemen; Alalmry1972@yahoo.com

† **Corresponding Author:** Dr. Govindaraju, Email: drgov@yahoo.com

ORCID: 0000-0002-0119-4826

Abstract: Flash floods are among the most dangerous natural disasters, as they cause widespread damage to property and loss of lives, especially in desert and mountainous areas. This study aims to evaluate Wadi Habban basin to be exposed to the risk of sudden floods using remote sensing data, geographic information systems (GIS), and the pyramid analysis methodology (AHP). The spatial distribution of hazardous areas has been evaluated through the weight and reclassification of ten main criteria that include: geomorphology, elevation, slope, rainfall, drainage density, distance to watercourse, land use and cover, soil texture, Topographic Wetness Index (TWI), and Stream Power Index (SPI), were integrated into a Geographic Information System (GIS) platform. The analysis classified basin into five risk categories: 4.3% (very high), 10.2% (high), 29.4% (medium), 42.2% (low), and 13.7%. (very low). The results revealed that 14.5% of the basin area is exposed to severe and high floods, which confirms the necessity of protective strategies, such as constructing flood barriers near vulnerable valleys, enhancing infrastructure and drainage systems. These results provide essential insights for disaster preparedness and infrastructure development, serving as a significant reference for policymakers and planners to enhance flood risk management and mitigate susceptibility in analogous settings.

Key Words	Flash flood susceptibility; Sensitivity analysis; analytical hierarchy process; Wadi Habban
DOI	https://doi.org/10.46488/NEPT.2025.v24i03.D4280 (DOI will be active only after the final publication of the paper)
Citation of the Paper	Haial Al-kordi, Abdulmohsen Al-Amri and Govinda raju, 2025. Flash Flood Susceptibility Mapping Using Geospatial And Analytical Hi-Erarchy Process Modeling - A Study Of Wadi Habban Basin, Shabwah, Yemen. *Nature Environment and Pollution Technology*, 24(3), B4280. https://doi.org/10.46488/NEPT.2025.v24i03.B4280

1. INTRODUCTION

Flooding, also known as inundation, is a significant hydrological disaster that ranks among the most destructive natural hazards globally, leading to substantial annual losses (Penki et al. 2023). This phenomenon can occur rapidly, often within a short period following intense precipitation, and is sometimes accompanied by secondary disasters such as landslides, mudflows, bridge failures, structural damage, and casualties (Hammami et al. 2019). Among the various forms of flooding, flash floods are particularly dangerous. The sudden, high-velocity flows result from intense rainstorms and frequently occur in coastal areas, alluvial fans, and mountainous valleys, inflicting severe damage and disruption to human activities. Population shifts caused by urbanization and unregulated growth have exacerbated the flash flood risk, which now affects basins of all sizes on every continent (Al-Areeq et al. 2023, Alarifi et al. 2022). In terrain conducive to rapid runoff, significant rainfall often triggers catastrophic flash floods (Costache et al. 2020). With over 70% of the global population living in flood-prone areas, the threat posed by flash floods is increasingly alarming (Al-Areeq et al. 2023). Each year, floods claim between 20 and 300 million lives worldwide and cause an estimated USD 60 million in economic losses. The increasing influence the result of climatic alteration, alterations in land use land cover, and continuous societal and economic development all suggest that an augmented risk of flooding will become more frequent and severe in the future. This highlights how critical it is to have precise flood assessments, techniques for mitigating damage, early warning systems, and efficient planning (Al-Areeq et al. 2023, Costache et al. 2020). Climate change, combined with urbanization and inadequate infrastructure, exacerbates the situation, with natural disasters, such as floods and droughts, becoming more common each year (Hammami et al. 2019). Developing nations, especially those with large agricultural sectors and limited disaster management capabilities, are particularly vulnerable to these disasters (Breisinger et al. 2012).

Yemen is an example of a disaster-prone country, facing numerous natural hazards annually. As reported by the Emergency Events Database (EM-DAT), more than 100,000 people in Yemen die annually due to natural disasters, with floods contributing significantly to economic and agricultural losses. Several climate models predict that increased precipitation will further intensify the frequency and severity of floods in Yemen (Al-Aizari et al. 2022).

Flooding in Yemen has severe economic repercussions and has considerably deteriorated living conditions. Floods intensify desertification and land degradation, resulting in agricultural losses, livestock fatalities, diminished availability of housing materials, famine, and heightened food insecurity. Yemen's dependence on agriculture and subsistence farming leaves it highly exposed to climate-related issues like flash floods. These events hinder food supply chains, raising the risk of famine (Mcfee 2024). Floodwaters often carry industrial waste and oil residues, worsening pollution and damaging farmland and vegetation (Al-Dailami et al. 2022). Additionally, these conditions increase the likelihood of diseases such as dengue fever, malaria, and cholera (ACAPS 2020, Semenza et al. 2022).

For instance, in October 2008, heavy rainfall led to devastating flooding in Wadi Hadramout. Rapid population growth, urbanization without proper regulation, and insufficient environmental controls have further heightened Yemen’s vulnerability to natural hazards (Breisinger et al. 2012). Due to changes of climatic conditions, the likelihood of flooding in the villages situated along the streams banks in the plains areas has raised significantly (Garg & Ananda Babu 2023). The rising frequency and severity of flooding and extreme precipitation events, exacerbated by climate change, are anticipated to intensify health and humanitarian issues in Yemen (Khalil & Thompson 2024).

In Shabwah Governorate, particularly in Wadi Habban region, frequent flood due to intense rainfall events, combined with geographical and hydrological factors, weak infrastructure, and limited its control measures, significantly increase flood risk. The study area has seen numerous flash floods in the past such as in the 1996 Oman cyclone, also known as (Cyclone 02A) (Maathuis et al. 1999), flash floods in Yemen in 2008, and Cyclone Chapala in 2015. In 2020, heavy rainfall severely impacted various governorates, particularly Hadhramaut, Shabwah, and Al Mahrah (UNISDR 2015).

The region's topography marked by vast desert plains, steep mountains, and rocky landscapes, along with human modifications in flood plains and catchments such as the erection of bridges, roads, and residences significantly leads to accelerated runoff and the occurrence of flash floods (Garg & Ananda Babu 2023). Natural disasters, being inevitable, require vigilant monitoring and the implementation of risk and vulnerability mitigation strategies, where the indicator creation tool is considered an essential element in flood management. Flood risk assessment is divided into three specific categories: exposure categories, vulnerability categories, and categories flood hazard (Oyebode & Paul 2023).

The accurate assessment of flood risks in Shabwah Governorate especially Wadi Habban basin, which represents one basins of the most importance for reducing and managing the risks posed by natural disasters. This study used GIS-based spatial analysis and the Analytical Hierarchy Process (AHP) to identify flood susceptibility zones in the basin, an area without previous studies on flash flood risk assessment. By concentrating on this particular basin, this research fills a critical knowledge gap and provides a methodological framework for addressing flood hazards in arid and semi-arid environments. This approach is important in its combination of AHP and GIS for the Wadi Habban basin, providing a replicable and scalable methodology for flood risk assessment in data scarce regions. This approach provides a comprehensive means to identify flood-prone areas by analyzing various factors, like rainfall patterns, topography, land use, and drainage networks. Subsequently flood hazard maps can be developed to inform policy decisions, enhance disaster preparedness, and promote sustainable land management.

The use of multi-criteria decision analysis (MCDA), geographic information systems (GIS), and remote sensing has proven effective in mapping flood-affected areas (Abdo et al. 2024, Corvacho-Ganahín et al. 2023). Remote sensing technology provides essential information about the distribution and behavior of floods. The proposed method was applied for the first time in Wadi Habban basin. The scientific outcomes of this research resulted in the creation of a flash flood susceptibility map, categorized into five levels: very high, high, moderate, low, and very low susceptibility. This map can assist planners, engineers, and government officials in developing appropriate strategies to prevent and mitigate future flooding events.

2. MATERIALS AND METHODS

The methodologies employed in the present study are illustrated in the flowchart in Fig.2.The fundamental purpose of this work is the identification of flood-prone sites using the GIS environment and analytical hierarchy process modeling (Goumrasa et al. 2021). These techniques were first applied in the Wadi Habban basin.

2.1. STUDY AREA

Wadi Habban basin is situated in the southeast part of the Shabwah Governorate of Yemen, as shown in (Fig. 1) between 14° 10′ and 14° 30′ N latitude and 46° 50′ and 47° 30′ E longitude, within the 38 UTM grid zone, including an area of approximately 1178.84 square kilometers. The elevation in the research area varies from 514 to 2108 meters above mean sea level (MSL). The study area is situated in an arid region, where floods frequently occur during the monsoon season as a result of heavy rainfall. It is this basin in Yemen is among basins those impacted by flash floods. Flash floods are a major problem in areas adjacent to a stream during the rainy season. The basin features a variety of terrains, including valleys, plains, mountains, and plateaus. The basin exhibits dendritic to sub-dendritic drainage patterns, showcasing moderate to high drainage textures. The study area's primary land use is agricultural, while there is some natural vegetation cover in sections of the basin. Residential areas are located near both sides of the valley, which may warn of potential flood. The climate of the region exhibits variability, characterized by hot summers and cold winters, accompanied by significant rainfall. The region's geology comprises sedimentary materials, such as sandstone and limestone that cover the middle and lower parts of the basin, while the top part of the basin is characterized by volcanic rocks, like granite. As well as the presence of steep and gentle slopes.

2.2. FLOOD INFLUENCING FACTORS

Figure 2 describes the research approach used in this work, which uses GIS and remote sensing data to identify locations that are prone to flooding. It also includes determining the "Flood Hazard Index (FHI)" by integrating the Analytic Hierarchy Process (AHP) with Multi-Criteria Decision-Making (MCDM) techniques, thereby forming a comprehensive framework for assessing flood risks. The use of AHP, recognized as one of the most effective methods for evaluating vulnerability to various natural disasters, is pivotal to the study. Its strength lies in its ability to consider the relative importance of multiple factors, providing a clear decision-making structure that enables decision-makers to derive information and effective conclusions.

In the study region, both climates, human and natural factors influence on the flood flow, various data sources were utilized as satellite imagery, a digital elevation model (DEM), climate data as well as spatial and geomorphological maps as data sources as shown in (Table 1), and processing using ArcGIS software, version number (ArcGIS 10.4) and ERDAS software, version number (ERDAS 2014). Furthermore, the research involved the selection of ten critical parameters essential for pinpointing flood-prone regions, including landforms, elevation, slope, drainage density, distance to the stream, land use/land cover (LULC), rainfall, soil texture, topographic wetness index (TWI), and stream power index (SPI).

The geomorphological map was created from two geomorphological maps supplied by the Department of Geology and Mineral Exploration in Yemen, after procedure georeferencing to them by ArcGIS software, version number (ArcGIS 10.4). The topographic gradient (slope), elevation values, drainage density, distance to stream, topographic wetness index (TWI), stream power index (SPI) were extracted from Digital Elevation Model (DEM) data. Utilizing the spatial analysis tools in ArcGIS software, version number (ArcGIS 10.4). We used monthly rainfall data; the annual mean rainfall was computed and obtained from the Global Rainfall data website, covering 20-years (from 2000 to 2020) (CRU TS v4.05 Data Variables, n.d.). Data on land use and land cover (LULC) were acquired from satellite images Landsat 8 from USGS Earth Explorer site and were processed utilizing supervised classification techniques in ERDAS software, version number (ERDAS 2014).

Created a soil texture from the FAO Digital Soil Map of the World (DSMW) by ArcGIS software, version number (ArcGIS 10.4).

2.3. ANALYTICAL HIERARCHY PROCESS (AHP) METHOD

2.3.1. Normalization and factor's weight evaluation

The method consists of three evaluation stages: constructing hierarchies, establishing priorities, and conducting evaluation using the consistency index (CI) (Saaty 1980). The AHP process encompasses the following sequential steps: (a) identification of influencing factors as components, (b) organization of these factors into a hierarchical structure, (c) allocation of numerical values to assess the relative significance of each factor, (d) development of a comparison matrix, (e) calculation of eigenvectors (final score), and (f) prioritization of alternatives (Makonyo & Zahor 2023). This method is advantageous for flood mapping as it readily identifies inconsistencies in judgment (Mudashiru et al. 2022). The elements have been standardized based on Saaty's 1 to 9 scale of relative importance (Table 2).

2.3.2. Pairwise Comparison Matrix (PCM) of Influence Factors

The Pairwise Comparison Matrix (PCM) is organized with factors ranked according to their respective impact on flood occurrence. The diagonal values must exert equal influence (equal to 1). The PCM of the matrix (μ) is computed by (Eq. 1) and as shown in (Table 4).

$$\mu = (aij)n * n = \begin{bmatrix} a11 & a12 & a1n \\ a21 & a22 & a2n \\ an1 & an2 & ann \end{bmatrix}, \text{aii=1, aij=1/aij, aij} \neq 0 \ \ldots\ldots\ldots\ldots\ldots\ldots\ldots\ldots\ldots\ldots\ldots \ (1)$$

Where, aij is the element at the (i) row and (j) column, (n*n) indicates the size of the square matrix (i.e., it has n rows and n columns), (aii) this states that all diagonal elements of the matrix are equal to 1, i.e., the importance of an element compared to itself is always equal to 1.

2.3.3. Calculation of the principal eigenvalue (λw)

The λw step helps measure the consistency of assessed weights (Saaty 1980). Appropriate weights are those with λw equal to or greater than the number of elements and a consistency ratio (CR) below 10% (0.1) (Saaty 1980). The present study found λw to be 10.01, surpassing the number of components (10).

2.3.4. Model consistency index (CI) computation

CI computation in the AHP technique evaluates weight assignment judgment. In (Eq. 2), CI is calculated by dividing λw by the number of elements assessed (n).

$$\mathrm{CI} = \frac{\lambda\mathrm{max} - \mathrm{n}}{\mathrm{n} - 1} \quad \ldots\ldots\ldots\ldots\ldots\ldots\ldots\ldots\ldots\ldots\ldots\ldots (2)$$

Whereas, λw =10.01 n=10 CI = 0.001

2.3.5. Calculating consistency ratio (CR)

The computation of CR utilizes the Random Index (RI) values established by Thomas Saaty see (Table 5). The RI values provide the index values derived from the number of factors assessed in the model (Saaty 1980). The computation of the CR is conducted as per (Eq.3).

$$\mathrm{CR} = \frac{\mathrm{CL}}{\mathrm{RI}} \quad \ldots\ldots\ldots\ldots\ldots\ldots\ldots\ldots\ldots\ldots\ldots\ldots (3)$$

Whereby, CI =0.001. RI=1.49 Therefore, CR = 0.0007% (Accepted).

2.3.6. Weighted Overlay combination (WOC) analysis

This research included ten factors to accurately assess and define the potential for flood susceptibility, and all parameters are converted to raster format, with the spatial resolution of each layer modified to a cell size of 30 m x 30 m, then division of each parameter into subclasses and using reclassification tool to that parameters and allocation of weights, as well as compute the flood hazard index based on the weights of the parameters by applying (Eq.4). The obtained data is additionally evaluated utilizing Geographic Information Systems (GIS).

$$\mathrm{FHI} = \sum_{i=1}^{n} Wi\ X\ Ri \quad \ldots\ldots\ldots\ldots\ldots\ldots\ldots\ldots\ldots\ldots\ldots\ldots (4)$$

Where, FHI refer to the flood hazard index, n refers to the number of parameters, Wi refers to the weighting factors, and Ri indicates the ratings of the factors.

These layers are then superimposed using ArcGIS, version number (ArcGIS 10.4) weighted overlay of spatial analysis tools, taking into account the effective weight derived from the AHP technique (Table 6). A database has been created for flash floods in the Wadi Habban basin, resulting in the created of a flash flood susceptibility map categorized into five levels: very high sensitivity, high sensitivity, moderate sensitivity, low sensitivity, and very low sensitivity.

3. RESULTS AND DISCUSSIONS

3.1. FLOOD RISK ASSESSMENT PARAMETERS

3.1.1. Geomorphological Map

Geomorphological analysis is essential for assessing the probability of flash flood events. It is crucial for managing water resources and assists in planning and development activities such as flood management and runoff reuse. The research region showcases five significant geomorphic features, as illustrated in (Fig 3a).

Wadi and floodplains: Very high susceptibility (101.38 km², which represents 8.6%), alluvial plains: High/moderate vulnerability (270 km², 23%), Plateaus: Low to moderate susceptibility (132.03 km², 11.2%) and Mountains and hills: Very low susceptibility (651.31 km², 55.25%), as shown in (Table 6).

Integrating geomorphological maps with flood susceptibility maps is a powerful approach to improving our understanding and management of flood risks.

3.1.2. Elevation Map

Elevation is an essential variable in flood risk assessment, directly affecting the flow and buildup of floodwaters. The low-lying locations are especially susceptible to flooding during inundation occurrences due to gravitational forces and topographical depressions, frequently serving as focal places for water accumulation and thus experiencing an elevated risk of flooding (Abdo et al. 2024). Previous research has shown that altitude has a significant influence on floods (Tehrany et al. 2019). The created map has five categories, as shown in (Table 6).

The lower elevations (<800 m) of sea level are very highly susceptible to floods (150.89 km², 12.8%), while High elevation (>1600 m) suggest that the area is very low flood sensitivity (71.56km2) shown in (Fig.3b).

3.1.3. Slope Map

The generation and redistribution of flooding are substantially affected by topography, with slope gradient serving as strong an indicator of surface sensitivity to floods (Wałęga et al. 2024). In general, low-slope areas experience greater flooding, as floodwaters can quickly drain into these regions, making them more susceptible to inundation (Alves et al. 2024). The slope map has been classified in a study area into five categories based on the degree of slope (Table 6).

Very low slopes (0 to 10 °) are very high susceptible to floods, indicating a higher risk, where area (502.78km^2) with percentage (42.7%) of basin, however very high slopes indicate very low susceptible of flooding (>82 °) covering area (41.4km2) with percentage (3.5%) as shown in (Fig.3c).

3.1.4. Rainfall Map

The relationship between rainfall and floods has been established by a large number of previous literature (Burn & Whitfield 2023). It is impossible to predict the exact degree to which rainfall increases lead to flooding (Jiang et al. 2023). In all environmental environments, precipitation can be considered the primary source of floods (Gao et al. 2023).

A mean annual rainfall map was generated using ArcGIS software, (version number (ArcGIS 10.4), and the precipitation scale was classified into five categories, as shown in (Fig. 3d).

The precipitation levels in the study area vary significantly, influencing flood susceptibility. Zones with precipitation exceeding 346 mm, which constitute 33.3% of the area, categorized as having a very highly susceptible to floods regions. Furthermore, regions receiving less than 284.4 mm of annual rainfall, accounting for 6.6% of the total area, experience very low precipitation and are consequently less affected by flooding, see in (Table 6).

3.1.5. Drainage Density

Drainage density is a critical factor in flood management, described as the river's length per square kilometer (km/km^2) (Al-Omari et al. 2024). The high drainage density refers to low filtration; conversely, high water filtration is indicated by low drainage density(Yang et al. 2022). The drainage density within the research area's topography exhibits significant variation, characterized by elevated densities in mid-slope and low elevation regions attributable to water convergence and soil infiltration, whereas steeper, higher-altitude zones demonstrate reduced drainage density. The drainage density in the study area is classified into five classes, as illustrated in (Fig. 4a).

The high drainage density (1.45 – 2.29 km/km^2), represent a very high flood susceptible regions covering an area of approximately 108.9 km^2, which 9.2% of the total region. Conversely, areas characterized by very low drainage density as mountains, hills, and plateaus, spanning 223 km^2 and accounting for 18.9% of the study area, exhibit low drainage densities (ranging from 0 to 0.38) and are very low flood susceptible, shown in (Table 6).

3.1.6. Distances from Stream

The locations nearest the streams source are those most susceptible to and affected by severe flash flooding. The flash flood severity will be highest in those areas when water flow exceeds that buffer zone (Hagos et al. 2022). As a result, the distance from the streams is given significant weight when establishing the flood potential zone.

The study area was divided into five zones based on proximity to streams using the buffer zone tool in ArcGIS, software (version 10.4) see in (Table 6).

The distance from stream (<100m) is classified as a very high flood risk zone, covering approximately 35.4 km^2, which is 3% of the all area, while the distance from stream (>800m) is classified as a very low flood risk zone, covering an area of 925.4 km^2, accounting for 78.5% of the region as shown in (Fig. 4b).

3.1.7. Land Use Land Cover (LULC)

Land use is important element in affecting areas susceptible to flooding plays a crucial role in water percolation, infiltration rate, and groundwater recharge (Xiao et al. 2024). Alterations in land use and land cover (LULC) can profoundly impact hydrological processes. The proliferation of impermeable surfaces in urban environments results in elevated surface runoff which increases the flow of flood activity there and diminished infiltration (Nwokeabia & Odinye 2024). With the expansion of the built area, the cover of the wetlands increases, while the cover of the plants diminishes, increasing the flow of water (Arya & Singh 2021, Hagos et al. 2022)

The classification of land use and land cover within Wadi Habban basin has been into seven categories, reflecting their potential impact on flood rates, as illustrated in (fig. 4c).

The study observed that the water bodies, closeness of infrastructure, built up expansion, and agricultural land near streams significantly increase the flood sensitivity, designating these locations as having a very high flood risk. In contrast, arid environments, such as highlands and hilly areas, are classified as having a very low flood risk (Table 6).

3.1.8. Soil Texture

In actuality, soil features such as structure and texture can significantly affect how permeable it is and, how much water storage is crucial in flood mapping (Costache et al. 2020).The three types of soil texture were produced (Table6).

Loam soil (medium texture), high susceptibility flood it's a cover area of about (783.9km^2), while sandy loam (moderate coarse texture), represent low susceptibility flood has a cover area of (87.2km^2) as shown in (Fig 4d).

3.1.9. Topographic Wetness Index

The topographic wetness index (TWI) measures the flow accumulation at each point within a drainage basin and the capacity of water to flow down a slope due to gravity (Fig. 4e). This feature refers to the condition of soil moisture (Selvam & Antony Jebamalai 2023), that has influenced runoff generation. The formula for TWI is typically represented as:

$$\mathrm{TWI} = \ln\left(\frac{\mathbf{A}}{\mathbf{tan(B)}}\right) \quad \text{...} \quad (5)$$

Where A represents the upstream contributing area and B is the slope of the terrain.

The potential for high index values to accumulate a significant amount of water is a result of the low slope, and the reverse is also true. Consequently, regions with elevated topographic wetness index (TWI) are at a greater risk of inundation. The topographic wetness index (TWI) map divides the basin into five distinct classes, as presented in (Fig. 4e).

Areas with a topographic wetness index (TWI) value (> 14) are classified as having a very high flood risk, covering approximately 20.28 km^2. In contrast, regions with a topographic wetness index value (< 5) are categorized as having a very low flood risk, covering an area of 259.3 km^2, as shown in (Table 6).

3.1.10. Stream Power Index (SPI)

It is possible to evaluate the potential for river erosion at a particular topographical area using the stream power index (SPI), which describes the relationship between the force of water flow and erosion (Jebur et al. 2014). In the field of research, elevated stream power index values indicate channels and steep gradients where erosion of the stream may occur, than the stream become able of transporting larger amounts of sediments during floods, this can lead to enhanced sediment deposition downstream or in floodplain areas, affecting flood water flow patterns and increasing flood risk. The classified of stream power index (SPI) into five categories, shown in (Table 6).

The negative low stream power index values indicate to high flood risk region, conversely the positive high stream power index (SPI) values indicate to low flood risk region as shown in (Fig 4f).

3.2. Flood Hazard Index (FHI)

The reclassify tool in ArcGIS software, version number (ArcGIS 10.4), was employed to reclassify the raster files (Figs. 3,4) in accordance with AHP classifications (Table 6) This process involved assigning weights and ranking each parameter and subclass. The Flood Hazard Susceptibility Index was calculated using the weighted overlay spatial analysis tool in ArcGIS 10.4 software, as outlined below:

$$FHI = \sum_{i=1}^{n} Wi\ x\ Ri \qquad \dots\dots\dots (6)$$

Where, n represents the number of parameters, Wi indicates the weight of each parameter, and Ri signifies the factor rating.

According to (Elkhrachy 2015), the flooding probability rate is assessed by the FHI and can be calculated using the subsequent equation:

FHI = 0.12(Geomorphological) + 0.13(Elevation) + 0.11(Slope) + 0.10(Rainfall) + 0.11 (Drainage density) + 0.12(Distance from stream) + 0.09(LULC) + 0.05(Soil texture) + 0.12(TWI) + 0.05(SPI).

3.3. The Flood Susceptibility Map

The ten maps were reclassified using ArcGIS software, version number (10.4), and then used the weighting approach and Analytic Hierarchy Process (AHP) to calculate weights. They were combined and superimposed in a GIS environment by spatial analysis tools then weighted overlay to find zones prone to floods (Mann & Gupta 2023). The final flood map obtained from the AHP approach divided the area into five categories, depending on the potential for flash floods from very high to very low, as shown in (Figs. 5, 6). According to the study area, 13.7% represents very low susceptibility, covering an area of 161.2 km^2, 42.4% represents low susceptibility, covering 500 km^2, 29.4% represents moderate susceptibility, covering 346.81 km^2, 10.2% represents high susceptibility, covering 119.2 km^2; and 4.3% represents very high susceptibility, covering 51.2 km^2, as shown in (Table 7).

Our analysis indicates that zones categorized as having high and very high susceptibility are at significant risk of flash flooding. The research area is characterized by high drainage density and low soil permeability, largely attributed to its topography of gentle slopes and low elevation. Additionally, the dendritic drainage pattern of the basin channels substantial water flow during heavy rainfalls, exacerbated by a high Topographic Wetness Index (TWI) and low Stream Power Index (SPI). Increased human activity in adjacent areas to wadi channel exacerbates flood risk, as infrastructure in the valley periphery obstructs natural water flow pathways. These factors align with the findings of previous studies that emphasized the importance of such indicators in flood mapping using the AHP approach by (Shawky & Hassan 2023, Radwan et al. 2019).

Precipitation in the elevated western, northwestern, and southwestern zones of the basin contributes significantly to runoff accumulation. These zones, characterized by steep slopes, rugged terrains, and substantial elevation differences, generate high runoff volumes that flow downstream into the Wadi Habban Basin, as illustrated in (Fig. 3a, b, and c). The presence of impermeable surfaces in these regions (Fig. 4d) further intensifies flood risks by preventing water infiltration and increasing surface runoff.

This interplay of factors underscores the importance of integrating topographic, hydrological, and anthropogenic parameters in flood susceptibility modeling, consistent with the approaches recommended in previous regional flood studies (Hagos et al. 2022).

These findings demonstrate the utility of AHP-based flood susceptibility mapping for identifying and mitigating flood-prone areas. In line with previous studies, our results emphasize the necessity of incorporating both natural and human-induced factors to develop effective flood risk management strategies tailored to the unique characteristics of the study region.

3.4. Figures, Tables and Schemes

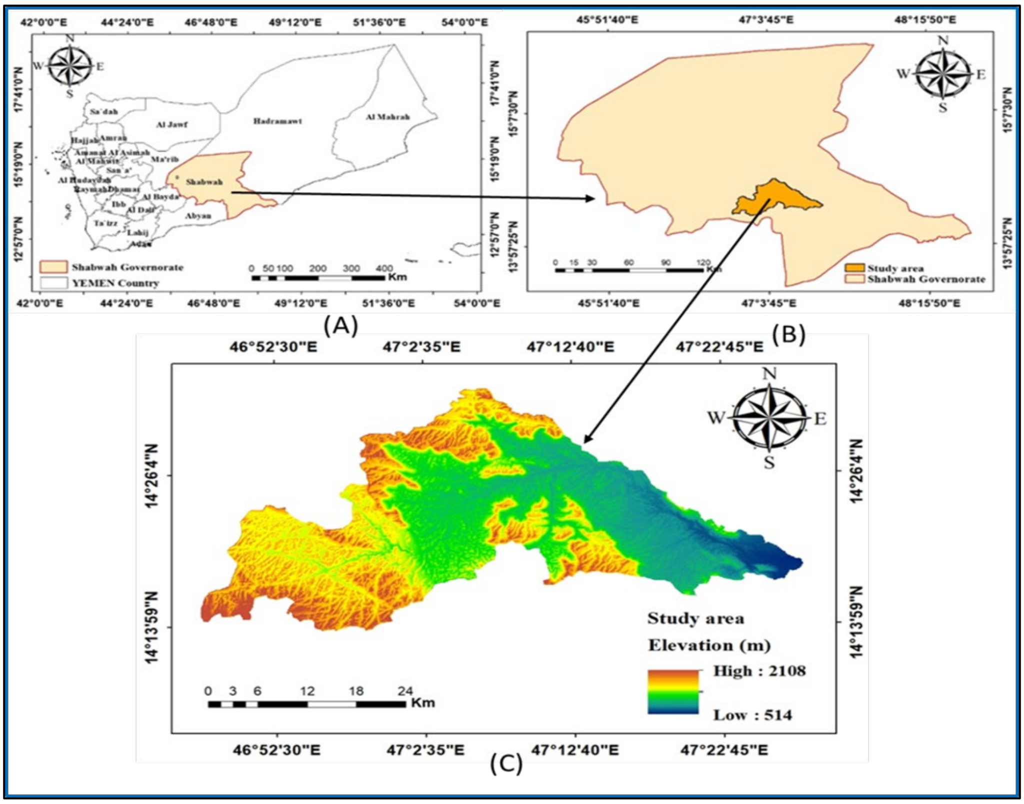

Fig. 1: (A) Yemen Country map, (B) Shabwah Governorate location map, (C) Wadi Habban Basin

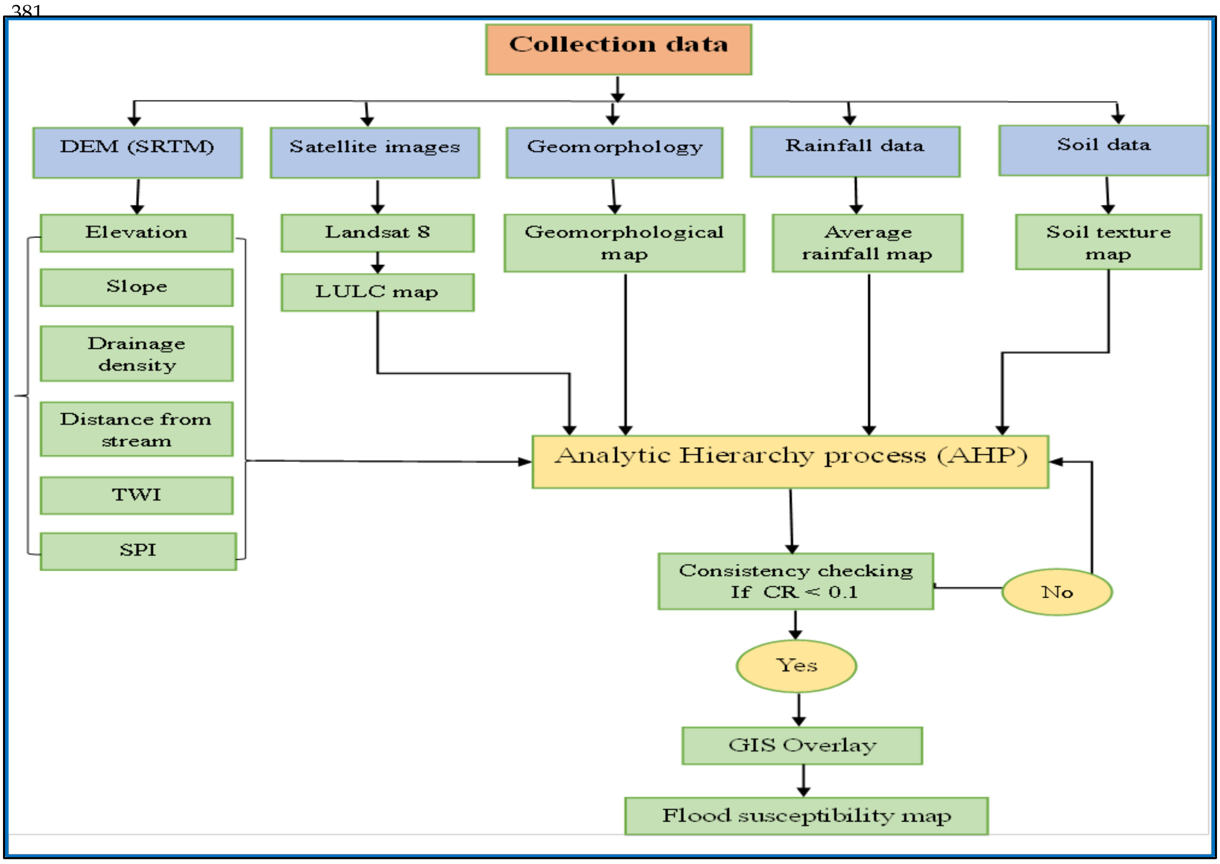

Fig. 2: The flow chart illustrates the methodology for the creation of maps of flood vulnerability maps in the research area.

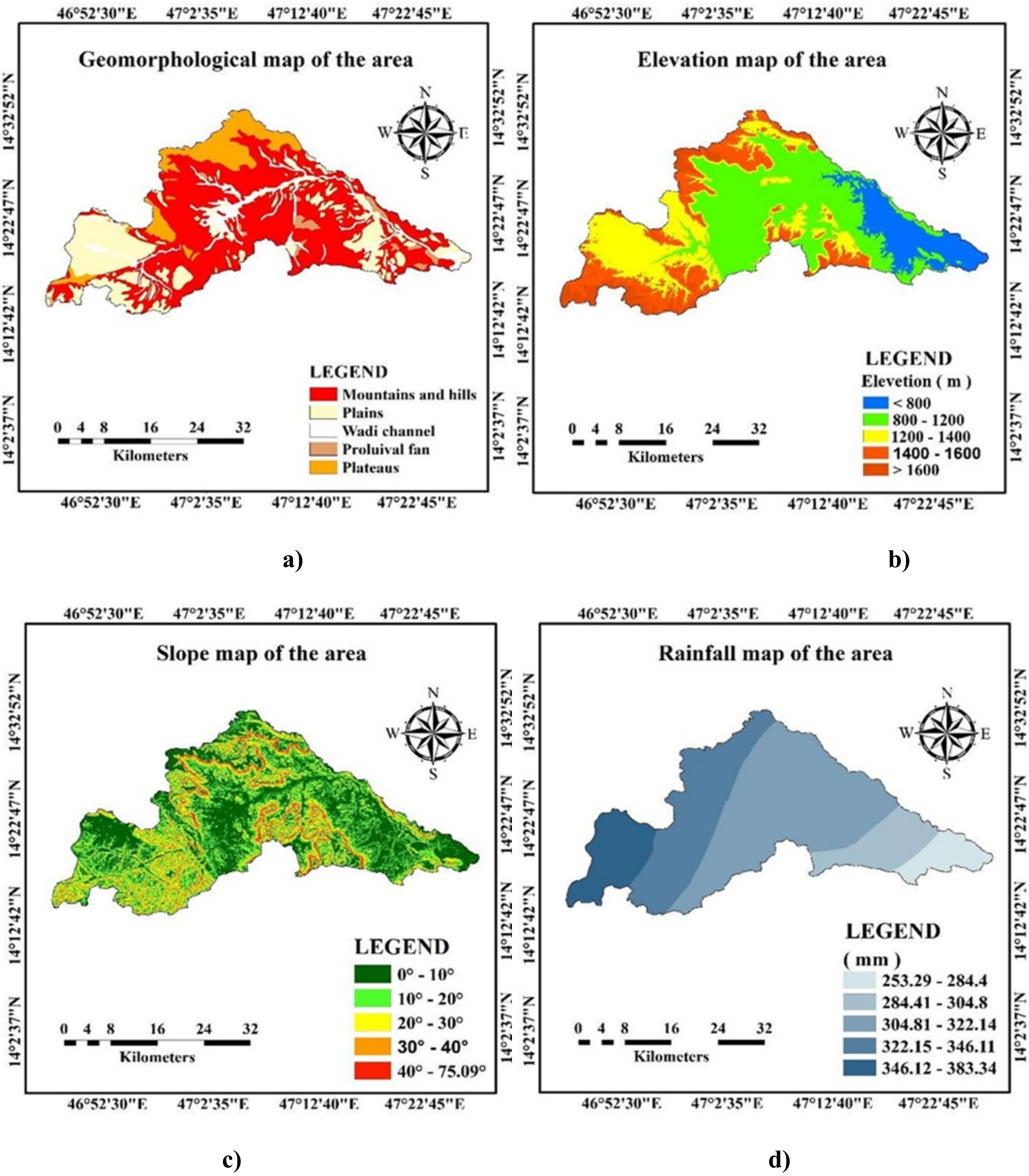

Fig. 3: a) Geomorphological map; b) Elevation map; c) Slope map; d) Rainfall map.

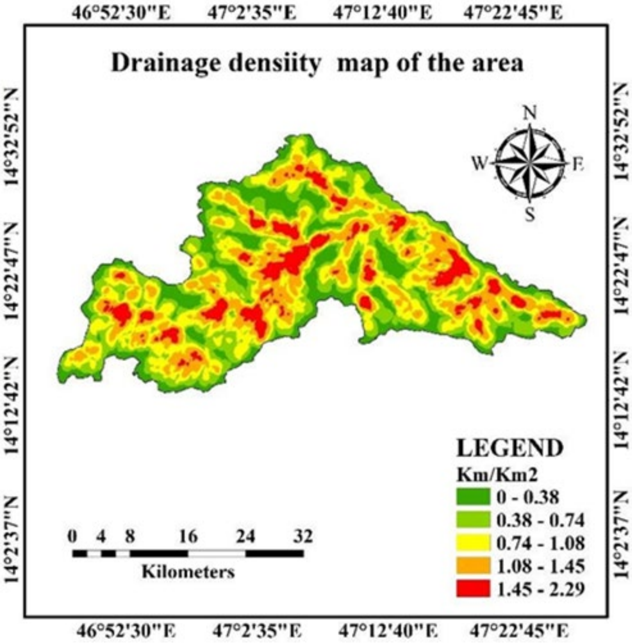

Drainage densiity map of the area
46°52'30"E
47°2'35"E
47°12'40"E
47°22'45"E
14°32'52"N
14°22'47"N
14°12'42"N
14°2'37"N
N
W
E
S
LEGEND
Km/Km2
0 - 0.38
0.38 - 0.74
0.74 - 1.08
1.08 - 1.45
1.45 - 2.29
0 4 8 16 24 32
Kilometers

a)

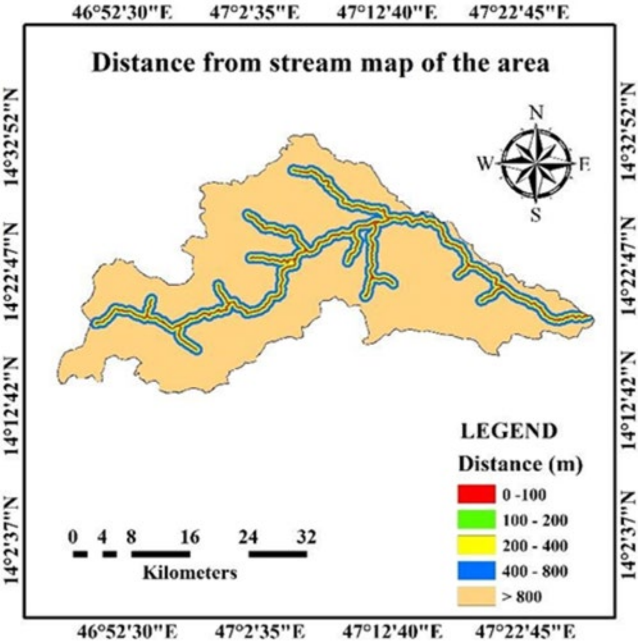

Distance from stream map of the area
46°52'30"E
47°2'35"E
47°12'40"E
47°22'45"E
14°32'52"N
14°22'47"N
14°12'42"N
14°2'37"N
N
W
E
S
LEGEND
Distance (m)
0 -100
100 - 200
200 - 400
400 - 800
> 800
0 4 8 16 24 32
Kilometers

b)

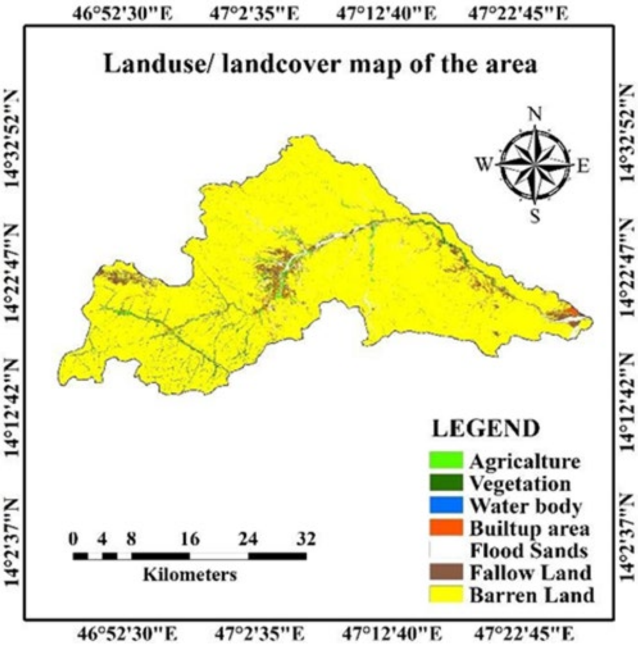

Landuse/ landcover map of the area
46°52'30"E
47°2'35"E
47°12'40"E
47°22'45"E
14°32'52"N
14°22'47"N
14°12'42"N
14°2'37"N
N
W
E
S
LEGEND
Agricalture
Vegetation
Water body
Builtup area
Flood Sands
Fallow Land
Barren Land
0 4 8 16 24 32
Kilometers

c)

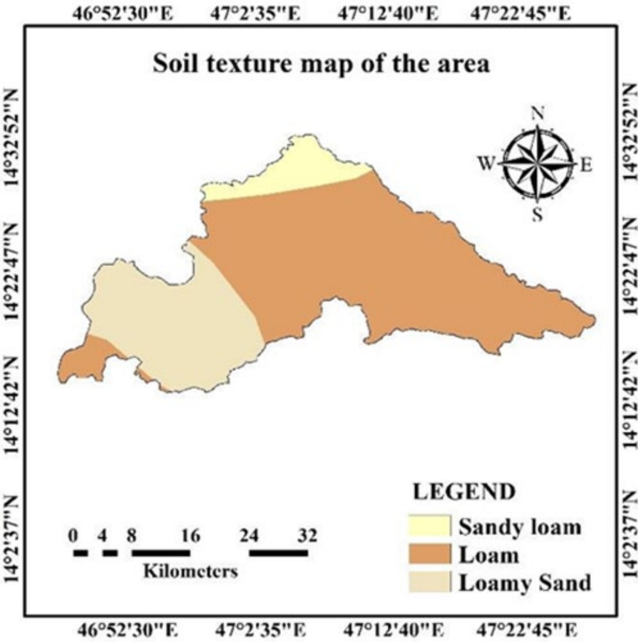

Soil texture map of the area
46°52'30"E
47°2'35"E
47°12'40"E
47°22'45"E
14°32'52"N
14°22'47"N
14°12'42"N
14°2'37"N
N
W
E
S
LEGEND
Sandy loam
Loam
Loamy Sand
0 4 8 16 24 32
Kilometers

d)

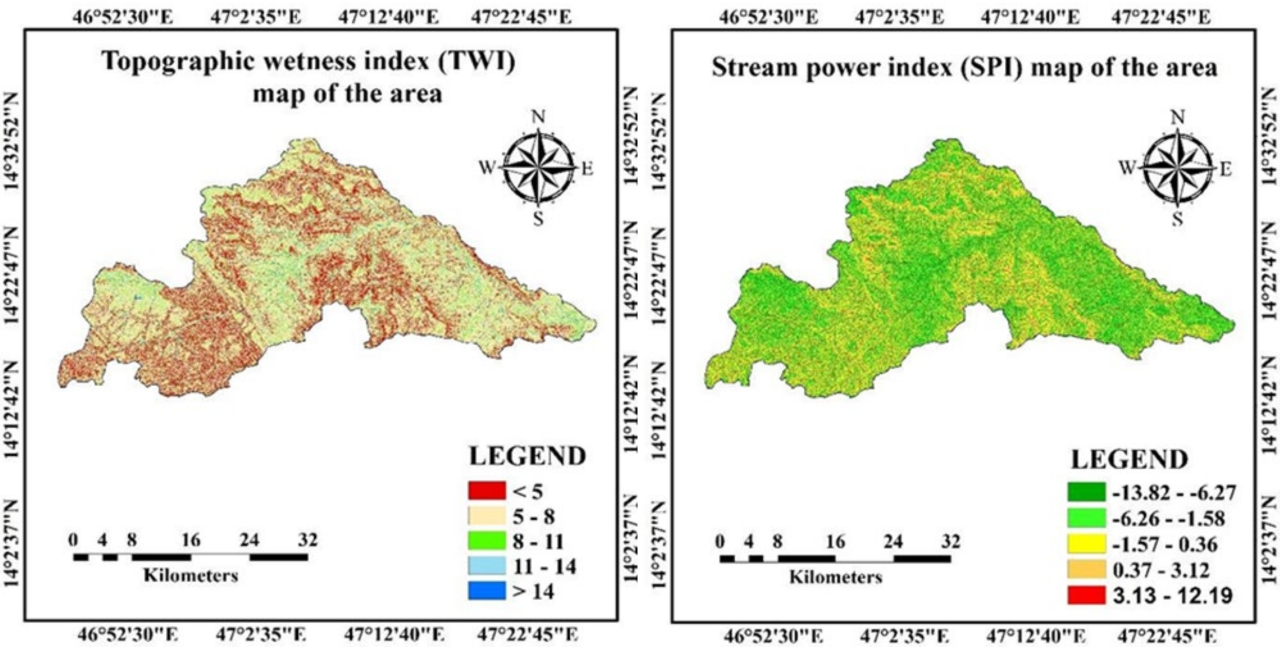

e) f)

Fig.4: a) Drainage density map; b) Distance from stream map; c) LULC map; d) Soil texture map; e) TWI map; f) stream power index (SPI) map.

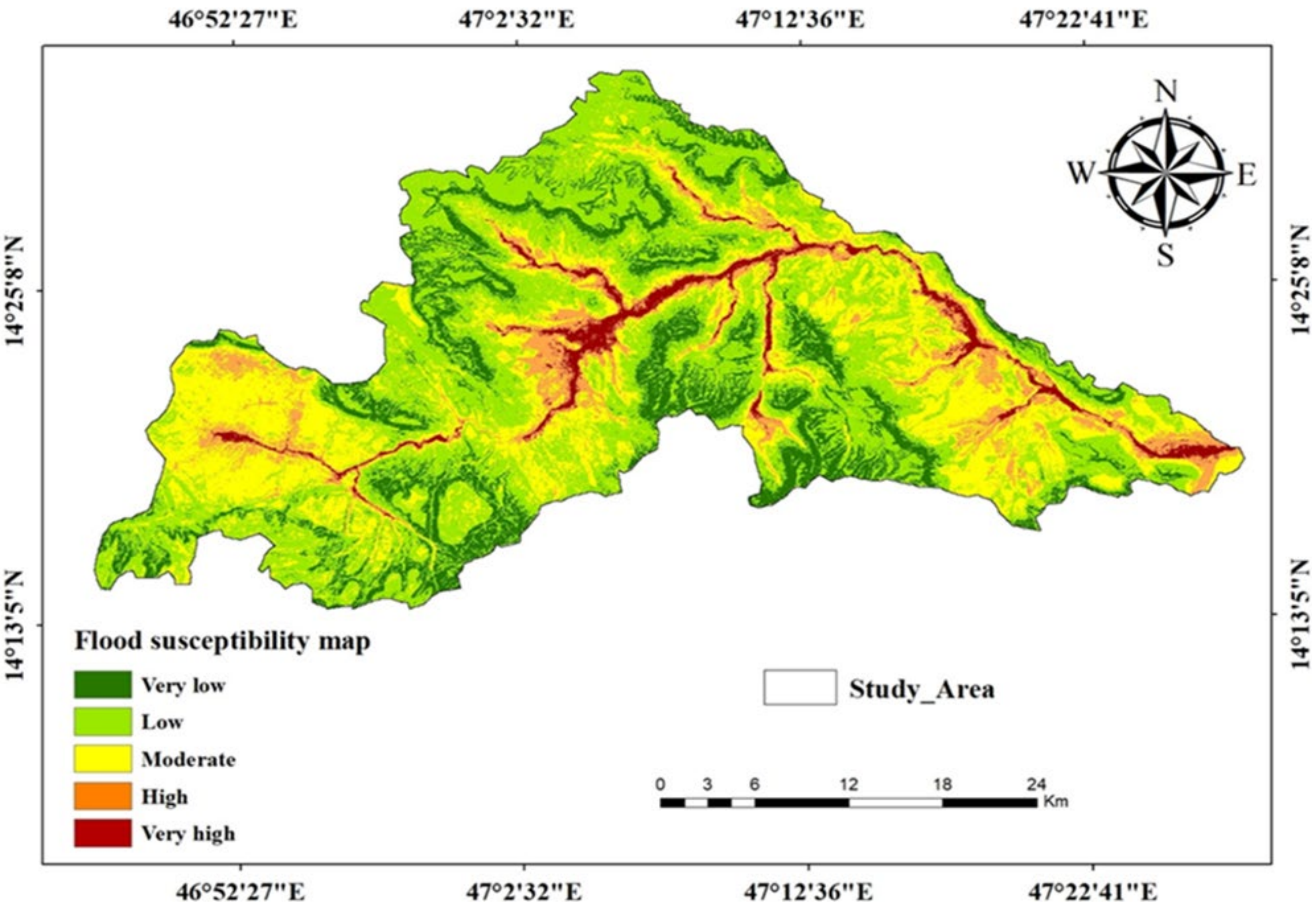

Fig.5: Flash flood hazard susceptibility map.

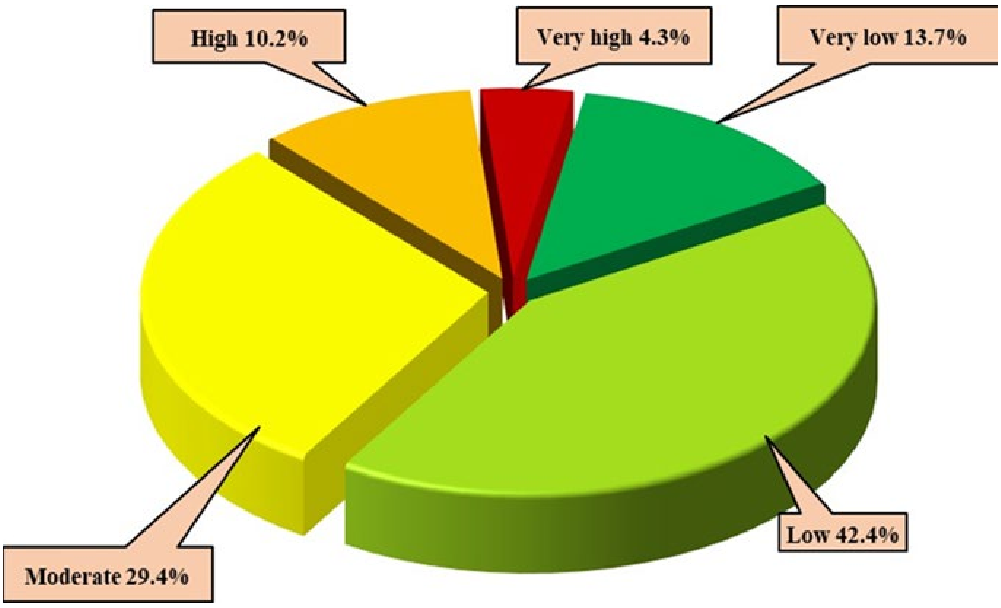

Fig.6: Distribution of flash flood susceptibility percentages

Table 1: Data sources for flood conditioning factors

Data Type	Source	Resolution /scale	Format	Purpose
Maps serial number of map (D38, D39)	Department of Geology and Mineral Exploration in Yemen	1:200000	Shapefile	Geomorphological map
Digital Elevation Model (DEM)	USGS Earth Explorer (SRTM) https://earthexplorer.usgs.gov	30m	TIFF	Extracting: slope, elevation, drainage density, distance to stream, TWI, SPI

Landsat 8 Imagery (05/10/2020)	USGS Earth Explorer https://earthexplorer.usgs.gov	30m	TIFF	Land use/land cover classification
Global Rainfall data website	Climatic Research Unit (CRU). https://crudata.uea.ac.uk/cru/data/hrg/	°0.5°×0.5° (~50 km)	TIFF	Rainfall distribution analysis.
Soil Data	FAO Soil Grids https://www.fao.org/soilsportal/data.	250m	GeoTIFF	Soil texture classification

Table 2: Shows Saaty's 1-9 scale for AHP (1980).

Level of preference	Preference scale	Inverse
Extremely significance	9	1/9
Very significant to extremely strongly	8	1/8
Very strongly Significantly	7	1/7
Strongly significant to very strongly	6	1/6
Strongly significant	5	1/5
Moderately significant to strongly	4	1/4
Moderately significant	3	1/3
Equally significant to moderately	2	1/2
Equally significant	1	1

Table 3: Random inconsistency index (RI)

n	3	4	5	6	7	8	9	10
RI	0.58	0.9	1.12	1.24	1.32	1.41	1.45	1.49

Table 4: Pairwise Comparison Matrix (PCM) of Influence Factors

Parameters	GE	EL	SL	RF	DD	DS	LULC	ST	TWI	SPI
GE	1.00	1.00	1.00	1.00	1.00	1.00	2.00	3.00	1.00	2.00
EL	1.00	1.00	1.00	2.00	1.00	1.00	2.00	3.00	1.00	2.00
SL	1.00	1.00	1.00	1.00	1.00	1.00	1.00	2.00	1.00	2.00
RF	1.00	1.00	0.50	1.00	1.00	1.00	1.00	2.00	1.00	2.00
DD	1.00	1.00	1.00	1.00	1.00	1.00	1.00	2.00	1.00	2.00
DS	1.00	1.00	1.00	1.00	1.00	1.00	1.00	3.00	1.00	3.00
LULC	0.50	1.00	0.50	1.00	1.00	1.00	1.00	2.00	0.50	2.00
ST	0.33	0.50	0.33	0.50	0.50	0.33	0.50	1.00	0.33	1.00
TWI	1.00	1.00	1.00	1.00	1.00	1.00	2.00	3.00	1.00	2.00
SPI	0.50	0.50	0.50	0.50	0.50	0.33	0.50	1.00	0.50	1.00

GE Geomorphological, **EL** Elevation, **SL** Slope, **RF** Rainfall, **DD** Drainage density, **DS** distance to stream, **LULC** Land use land cover, **St** Soil texture, **TWI** Topographic wetness index, **SPI** Stream power index.

Table 5: Normalized matrix with weights, to consistency ratio (CR) computation

Parameters	GE	EL	SL	RF	DD	DS	LULC	ST	TWI	SPI	criteria weight	Ratio
GE	0.015	0.015	0.014	0.010	0.012	0.014	0.015	0.006	0.015	0.006	0.12	0.99
EL	0.015	0.015	0.014	0.020	0.012	0.014	0.015	0.006	0.015	0.006	0.13	0.99
SL	0.015	0.015	0.014	0.010	0.012	0.014	0.008	0.004	0.015	0.006	0.11	1.02
RF	0.015	0.015	0.007	0.010	0.012	0.014	0.008	0.004	0.015	0.006	0.10	1.02
DD	0.015	0.015	0.014	0.010	0.012	0.014	0.008	0.004	0.015	0.006	0.11	1.02
DS	0.015	0.015	0.014	0.010	0.012	0.014	0.008	0.006	0.015	0.008	0.12	0.98

LULC	0.007	0.015	0.007	0.010	0.012	0.014	0.008	0.004	0.007	0.006	0.09	0.99
ST	0.005	0.007	0.005	0.005	0.006	0.005	0.004	0.002	0.005	0.003	0.05	0.99
TWI	0.015	0.015	0.014	0.010	0.012	0.014	0.015	0.006	0.015	0.006	0.12	0.99
SPI	0.007	0.007	0.007	0.005	0.006	0.005	0.004	0.002	0.007	0.003	0.05	1.01

GE Geomorphological, **EL** Elevation, **SL** Slope, **RF** Rainfall, **DD** Drainage density, **DS** distance to stream, **LULC** Land use land cover, **St** Soil texture, **TWI** Topographic wetness index, **SPI** Stream power index.

Table 6: Criteria and subcategories of factors with associated weights

Flood causative criterion	Classes	Area Km^2	Percentage %	Flood influence	Rating	Classes weight	Criteria weight
Geomorphology	Mountains and hills	651.3	55.25	Very low	1	0.12	**12**
	Plains	270	23	High	7	0.84	
	Wadi channel, flood plains	101.38	8.6	Very high	9	1.08	
	Proluival fan	24.16	2.05	Moderate	5	0.60	
	Plateaus	132.03	11.2	Low	3	0.36	
Elevation (m)	< 800	150.89	12.8	Very low	7	0.91	**13**
	800 - 1200	460.34	39.05	Low	5	0.65	
	1200 - 1400	283.51	24.05	Moderate	3	0.39	
	1400 - 1600	212.54	18.03	High	2	0.26	
	> 1600	71.56	6.07	Very high	1	0.13	
Slope degree	0 - 10	502.78	42.65	Very low	7	0.77	**11**
	10 - 20	315.93	26.8	Low	5	0.55	
	20 - 30	211.95	17.98	Moderate	3	0.33	
	30 - 40	106.8	9.06	High	2	0.22	
	40 - 75.09	41.38	3.51	Very high	1	0.11	

Rainfall (mm)	< 284	75.68	6.42	Very low	1	0.1	**10**
	285 - 305	124.49	10.56	Low	2	0.2	
	306 - 322	538.49	45.68	Moderate	3	0.3	
	323 - 346	298.13	25.29	High	4	0.4	
	> 347	142.05	12.05	Very high	5	0.5	
Drainage density (Km/Km^2)	0 – 0.38	223.04	18.92	Very low	1	0.11	**11**
	0.38 – 0.74	286.1	24.27	Low	2	0.22	
	0.74 – 1.08	300.84	25.52	Moderate	3	0.33	
	1.08 – 1.45	259.94	22.05	High	5	0.55	
	1.45 – 2.29	108.92	9.24	Very high	7	0.77	
Distance from stream (m)	0 - 100	35.36	3	Very high	9	1.08	**12**
	100 - 200	35.36	3	High	7	0.84	
	200 - 400	64.84	5.5	Moderate	5	0.60	
	400 - 800	117.88	10	Low	3	0.36	
	> 800	925.4	78.5	Very low	1	0.12	
LULC	Vegetation area	20.16	1.71	Very low	1	0.09	**9**
	Agriculture land	25	2.12	Moderate	5	0.45	
	Built-up area	34.3	2.91	High	7	0.63	
	Barren land	1030.43	87.41	Low	2	0.18	
	Fallow land	26.41	2.24	Moderate	5	0.45	
	Water body	4.95	0.42	Very high	9	0.81	
	Flood sands	37.49	3.18	High	7	0.63	
Soil texture	Sandy loam	87.23	7.4	Very low	1	0.05	**5**
	Loam	783.9	66.5	High	3	0.15	
	Loamy sand	307.7	26.1	Low	2	0.1	
	< 5	259.34	22	Very low	1	0.12	

TWI	5 - 8	726.87	61.66	Low	3	0.36	**12**
	8 - 11	123.78	10.5	Moderate	5	0.60	
	11 - 14	48.57	4.12	High	7	0.84	
	> 14	20.28	1.72	Very high	9	1.08	
SPI	3.13 – 12.2	40.79	3.46	Very high	9	0.45	**5**
	0.36 – 3.12	167.75	14.23	High	7	0.35	
	-1.57 - 0.36	360.96	30.62	Moderate	5	0.25	
	-6.26 - -1.58	205	17.39	Low	3	0.15	
	-13.8 - -6.27	449354	34.3	Very low	1	0.05	

Table 7: Classification of food susceptibility and their spatial distribution

NO.	Flood susceptibility classification	Area covered (Sq.km)	Percentage%
1	Very low susceptibility	161.2	13.7 %
2	Low susceptibility	500	42.4%
3	Moderate susceptibility	346.81	29.4%
4	High susceptibility	119.8	10.2%
5	Very high susceptibility	51.2	4.3%

4. CONCLUSIONS

The assessment of flood hazard zones is a crucial element of a flood control strategy; the suggested methodology was implemented in Wadi Habban basin for the purpose of mapping the flash flood, the integration of geographic information systems (GIS) with multi criteria spatial assessment and the analytic hierarchy process (AHP) has proven to be highly effective in supporting decision-making processes, as this approach takes into account the significant impact of multiple factors contributing to occurrence flooding in the region. Ten distinct input maps have been generated, including geomorphological, elevation, slope, drainage density, distance to the stream, land use/land cover (LULC), rainfall, soil texture, topographic wetness index (TWI), and stream power index (SPI). The research found that topography (elevations, slopes, and valleys), proximity to stream, topographic wetness index (TWI), heavy rainfall, drainage density and land use are the primary factors contributing significantly to flood occurrence in the region, whereas soil texture and stream power index (SPI) had a lesser influence.

Based on flood sensitivity, which ranges from very low to very high, the flash flood susceptibility maps of the Wadi Habban Basin were classified into five major categories: 13.7% (very low), 42.4% (low), 29.4% (moderate), 10.2% (high), and 4.3% (very high), as shown in (Fig.5), (Table 7). The study concluded that several residential areas near the valley course are at risk of flash floods if the valley cannot absorb the water during heavy rain seasons. These areas include the Al-Said region, Habban, parts of Lahiya, Al-Ghil, Lamatir, and sections of Azzan City.

The final findings enhance our understanding of the relationship between topographic, hydrological, geological, and climatic factors and flash flood conditions. The research demonstrated that the technologies employed, as remote sensing and geographic information systems (GIS) were reliable and effective. These technologies will help planners identify dangerous areas, protect local residents, and improve disaster response after heavy rains.

To reduce flash flood risks in the Wadi Habban basin, authorities and international organizations should use Geographic Information Systems (GIS) to create detailed flood hazard maps, identifying the most vulnerable areas. These maps can guide key measures such as implementing early warning systems, constructing check dams, and improving drainage infrastructure. Collaboration with international experts can provide the technical and financial support needed for sustainable solutions that also address climate change impacts. Future studies should incorporate real-time hydrological data, examine long-term climatic trends, and utilize machine learning to effective flood risk management in the region. Social and economic data collection will enhance vulnerability assessments, while interactive risk maps and 3D simulations can improve planning. These efforts will provide comprehensive tools for effective flood risk management in the region.

Funding: “This research received no external funding”.

Conflict of Interest: The authors declare no conflict of interest.

REFERENCES

Abdo, H. G., Darwish, K. S., Bindajam, A. A., Niknam, A., Youssef, Y. M., Ahmed, M. F. M., & Mallick, J. (2024). Detection of flood vulnerable areas in urban basins using multi-criteria analysis and geospatial tools: a case study from eastern Mediterranean. Environmental Earth Sciences, 83(17), 1–20. https://doi.org/10.1007/s12665-024-11801-0

Abdo, H. G., Zeng, T., Alshayeb, M. J., Prasad, P., Ahmed, M. F. M., Albanai, J. A., Alharbi, M. M., & Mallick, J. (2024). Multi-criteria analysis and geospatial applications-based mapping flood vulnerable areas: a case study from the eastern Mediterranean. Natural Hazards, 0123456789. https://doi.org/10.1007/s11069-024-06864-y

ACAPS. (2020). Yemen - Heavy rainfall and flash floods. ACAPS Yemen Analysis Hub.

Al-Aizari, A. R., Al-Masnay, Y. A., Aydda, A., Zhang, J., Ullah, K., Islam, A. R. M. T., Habib, T., Kaku, D. U., Nizeyimana,

J. C., Al-Shaibah, B., Khalil, Y. M., AL-Hameedi, W. M. M., & Liu, X. (2022). Assessment Analysis of Flood Susceptibility in Tropical Desert Area: A Case Study of Yemen. Remote Sensing, 14(16). https://doi.org/10.3390/rs14164050

Al-Areeq, A. M., Abba, S. I., Halder, B., Ahmadianfar, I., Heddam, S., Demir, V., Kilinc, H. C., Farooque, A. A., Tan, M. L., & Yaseen, Z. M. (2023). Flood Subsidence Susceptibility Mapping using Elastic-net Classifier: New Approach. Water Resources Management, 37(13), 4985–5006. https://doi.org/10.1007/s11269-023-03591-0

Al-Dailami, A., Ahmad, I., Kamyab, H., Abdullah, N., Iwamoto, K., Veeramuthu, A., & Zabara, B. (2022). Sustainable solid waste management in Yemen: environmental, social aspects, and challenges. Biomass Conversion and Biorefinery, 1–27. https://doi.org/10.1007/s13399-022-02871-w

Al-Omari, A. A., Shatnawi, N. N., Shbeeb, N. I., Istrati, D., Lagaros, N. D., & Abdalla, K. M. (2024). Utilizing Remote Sensing and GIS Techniques for Flood Hazard Mapping and Risk Assessment. Civil Engineering Journal (Iran), 10(5), 1423–1436. https://doi.org/10.28991/CEJ-2024-010-05-05

Alarifi, S. S., Abdelkareem, M., Abdalla, F., & Alotaibi, M. (2022). Flash Flood Hazard Mapping Using Remote Sensing and GIS Techniques in Southwestern Saudi Arabia. Sustainability (Switzerland), 14(21). https://doi.org/10.3390/su142114145

Alves, R. A., Rudke, A. P., de Melo Souza, S. T., dos Santos, M. M., & Martins, J. A. (2024). Flood vulnerability mapping in an urban area with high levels of impermeable coverage in southern Brazil. Regional Environmental Change, 24(3), 1–16. https://doi.org/10.1007/s10113-024-02258-9

Arya, A. K., & Singh, A. P. (2021). Multi criteria analysis for flood hazard mapping using GIS techniques: a case study of Ghaghara River basin in Uttar Pradesh, India. Arabian Journal of Geosciences, 14(8). https://doi.org/10.1007/s12517-021-06971-1

Breisinger, C., Ecker, O., Thiele, R., & Wiebelt, M. (2012). The Impact of the 2008 Hadramout Flash Flood in Yemen on Economic Performance and Nutrition: A Simulation Analysis. Kiel Working Paper, No. 1758(April 2014), 1–28. http://hdl.handle.net/10419/55865

Burn, D. H., & Whitfield, P. H. (2023). Climate related changes to flood regimes show an increasing rainfall influence. Journal of Hydrology, 617, 129075.

Corvacho-Ganahín, O., González-Pacheco, M., Francos, M., & Carvalho, F. (2023). Evaluation of potential flood hazard through spatial zoning in Acha–Arica, northern Chile, integrating GIS, multi-criteria analysis and two-dimensional numerical simulation. Natural Hazards, 118(1), 755–783. https://doi.org/10.1007/s11069-023-06027-5

Costache, R., Hong, H., & Pham, Q. B. (2020). Comparative assessment of the flash-flood potential within small mountain catchments using bivariate statistics and their novel hybrid integration with machine learning models. Science of the Total Environment, 711, 134514. https://doi.org/10.1016/j.scitotenv.2019.134514

CRU TS v4.05 Data Variables. (n.d.). Retrieved October 24, 2024, from https://crudata.uea.ac.uk/cru/data/hrg/cru_ts_4.05/cruts.2103051243.v4.05/

Elkhrachy, I. (2015). Flash Flood Hazard Mapping Using Satellite Images and GIS Tools: A case study of Najran City, Kingdom of Saudi Arabia (KSA). Egyptian Journal of Remote Sensing and Space Science, 18(2), 261–278. https://doi.org/10.1016/j.ejrs.2015.06.007

Gao, L., Zhang, L., Hong, Y., Chen, H.-X., & Feng, S.-J. (2023). Flood hazards in urban environment. Georisk: Assessment and Management of Risk for Engineered Systems and Geohazards, 17(2), 241–261. https://doi.org/10.1080/17499518.2023.2201266

Garg, C., & Ananda Babu, K. (2023). Extreme Flood Calibration and Simulation Using a 2D Hydrodynamic Model Under a Multipurpose Reservoir. Nature Environment and Pollution Technology, 22(2), 977–983. https://doi.org/10.46488/NEPT.2023.v22i02.042

Goumrasa, A., Guendouz, M., Guettouche, M. S., & Belaroui, A. (2021). Flood hazard susceptibility assessment in Chiffa wadi watershed and along the first section of Algeria North–South highway using GIS and AHP method. Applied Geomatics, 13(4), 565–585. https://doi.org/10.1007/s12518-021-00381-4

Hagos, Y. G., Andualem, T. G., Yibeltal, M., & Mengie, M. A. (2022). Flood hazard assessment and mapping using GIS integrated with multi-criteria decision analysis in upper Awash River basin, Ethiopia. Applied Water Science, 12(7), 1–18. https://doi.org/10.1007/s13201-022-01674-8

Hammami, S., Dlala, M., Zouhri, L., Souissi, D., Souei, A., Zghibi, A., & Marzougui, A. (2019). Application of the GIS based multi-criteria decision analysis and analytical hierarchy process (AHP) in the flood susceptibility mapping (Tunisia). Arabian Journal of Geosciences, 12, 1–16.

Jebur, M. N., Pradhan, B., & Tehrany, M. S. (2014). Optimization of landslide conditioning factors using very high-resolution airborne laser scanning (LiDAR) data at catchment scale. Remote Sensing of Environment, 152, 150–165. https://doi.org/10.1016/j.rse.2014.05.013

Jiang, X., Zhang, L., Liang, Z., Fu, X., Wang, J., Xu, J., Zhang, Y., & Zhong, Q. (2023). Study of early flood warning based on postprocessed predicted precipitation and Xinanjiang model. Weather and Climate Extremes, 42(September), 100611. https://doi.org/10.1016/j.wace.2023.100611

Khalil, A. H., & Thompson, S. (2024). Climate Change, Food Security and Agricultural Extension in Yemen. Journal of Rural and Community Development, 19(3).

Maathuis, B. H. P., Timmermans, W. J., & Meijerink, A. M. J. (1999). Short term assessment of the June 1996 flash-floods in Yemen. Geocarto International, 14(2), 29–33. https://doi.org/10.1080/10106049908542101

Makonyo, M., & Zahor, Z. (2023). GIS-based analysis of landslides susceptibility mapping: a case study of Lushoto district, north-eastern Tanzania. In Natural Hazards (Vol. 118, Issue 2). Springer Netherlands. https://doi.org/10.1007/s11069-023-06038-2

Mann, R., & Gupta, A. (2023). Mapping flood vulnerability using an analytical hierarchy process (AHP) in the Metropolis of Mumbai. In Environmental Monitoring and Assessment (Vol. 195, Issue 12). Springer International Publishing. https://doi.org/10.1007/s10661-023-12141-5

Mcfee, E. K. (2024). REPORT ON MIGR ATION , ENVIRONMENT , AND. April.

Mudashiru, R., Sabtu, N., Abdullah, R., Saleh, A., & Abustan, I. (2022). Optimality of flood influencing factors for flood hazard mapping: An evaluation of two multi-criteria decision-making methods. Journal of Hydrology, 612, 128055. https://doi.org/10.1016/j.jhydrol.2022.128055

Nwokeabia, B. I., & Odinye, C. N. (2024). Impact of Land Use and Land Cover Changes on Hydrological Characteristics and Drainage Density in Urban and Semi-Urban Areas of Abia State , Southeastern Nigeria. August. https://doi.org/10.56201/rjpst.v7.no3.2024.pg147.163

Oyebode, O. J., & Paul, F. (2023). Flood Mitigation and Pollution Abatement in Kaduna Metropolis Through Engineering Assessment and Analytical Hierarchy Process Design. Nature Environment and Pollution Technology, 22(2), 789–801. https://doi.org/10.46488/NEPT.2023.v22i02.021

Penki, R., Basina, S. S., & Tanniru, S. R. (2023). Application of geographical information system-based analytical hierarchy process modeling for flood susceptibility mapping of Krishna District in Andhra Pradesh. Environmental Science and Pollution Research, 30(44), 99062–99075. https://doi.org/10.1007/s11356-022-22924-x

Radwan, F., Alazba, A. A., & Mossad, A. (2019). Flood risk assessment and mapping using AHP in arid and semiarid regions. Acta Geophysica, 67(1), 215–229. https://doi.org/10.1007/s11600-018-0233-z

Saaty, T. L. (1980). The analytic hierarchy process. mcgrawhill international. New York.

Selvam, R. A., & Antony Jebamalai, A. R. (2023). Application of the analytical hierarchy process (AHP) for flood susceptibility mapping using GIS techniques in Thamirabarani river basin, Srivaikundam region, Southern India. Natural Hazards, 118(2), 1065–1083. https://doi.org/10.1007/s11069-023-06037-3

Semenza, J. C., Rocklöv, J., & Ebi, K. L. (2022). Climate Change and Cascading Risks from Infectious Disease. Infectious Diseases and Therapy, 11(4), 1371–1390. https://doi.org/10.1007/s40121-022-00647-3

Shawky, M., & Hassan, Q. K. (2023). Geospatial Modeling Based-Multi-Criteria Decision-Making for Flash Flood Susceptibility Zonation in an Arid Area. Remote Sensing, 15(10). https://doi.org/10.3390/rs15102561

Tehrany, M. S., Jones, S., & Shabani, F. (2019). Identifying the essential flood conditioning factors for flood prone area mapping using machine learning techniques. Catena, 175(December 2018), 174–192. https://doi.org/10.1016/j.catena.2018.12.011

UNISDR. (2015). Cyclone Chapala Disaster Risk Reduction Situation Report Summary report. PreventionWeb, 1–9.

Wałęga, A., Wojkowski, J., Sojka, M., Amatya, D., Młyński, D., Panda, S., & Caldvell, P. (2024). Exploiting satellite data for total direct runoff prediction using CN-based MSME model. Science of The Total Environment, 908, 168391.

Xiao, J., Xie, B., Zhou, K., Li, W., Liang, C., Li, J., Xie, J., Zhang, X., & Pang, X. (2024). Responses of hydrological processes to vegetation greening and climate change in subtropical watersheds. Journal of Hydrology: Regional Studies, 55(July), 101946. https://doi.org/10.1016/j.ejrh.2024.101946

Yang, S. Y., Chang, C. H., Hsu, C. T., & Wu, S. J. (2022). Variation of uncertainty of drainage density in flood hazard mapping assessment with coupled 1D–2D hydrodynamics model. Natural Hazards, 111(3), 2297–2315. https://doi.org/10.1007/s11069-021-05138-1